Author(s): Havu, P. & Puska, M. J. & Nieminen, Risto M. & Havu, V.

Title: Electron transport through quantum wires and point contacts

Year: 2004

Version: Final published version

Please cite the original version:

Havu, P. & Puska, M. J. & Nieminen, Risto M. & Havu, V. 2004. Electron transport through quantum wires and point contacts. Physical Review B. Volume 70, Issue 23. 233308/1-4. ISSN 1550-235X (electronic). DOI: 10.1103/physrevb.70.233308.

Electron transport through quantum wires and point contacts

P. Havu, M. J. Puska, and R. M. Nieminen
Laboratory of Physics, Helsinki University of Technology, P. O. Box 1100, FIN-02015 HUT, Finland

V. Havu
Institute of Mathematics, Helsinki University of Technology, P. O. Box 1100, FIN-02015 HUT, Finland
(Received 31 May 2004; revised manuscript received 9 September 2004; published 17 December 2004)

We have studied quantum wires using the Green's function technique within density-functional theory, calculating electronic structures and conductances for different wire lengths, temperatures, and bias voltages. For short wires, i.e., quantum point contacts, the zero-bias conductance shows as a function of the gate voltage and at a finite temperature a plateau at around $0.7G_0$. ($G_0=2e^2/h$ is the quantum conductance.) The behavior, which is caused in our mean-field model by spontaneous spin polarization in the constriction, is reminiscent of the so-called 0.7 anomaly observed in experiments. In our model the temperature and the wire length affect the conductance–gate-voltage curves similarly as in experiments.

DOI: 10.1103/PhysRevB.70.233308 PACS number(s): 73.63.Nm, 73.21.Hb

Interesting two-dimensional (2D) nanostructures can be fabricated at semiconductor interfaces (e.g., GaAs/AlGaAs) using lithographic techniques and gate electrodes. For example, quantum wires (QW's) and quantum point contacts (QPC's) are laterally narrow electron pathways connecting two (infinite) electrodes. In the regime of ballistic electron transport the conductance of QW's and QPC's is quantized in steps of $G_0=2e^2/h$. However, QPC's exhibit as a function of the gate voltage also the so-called 0.7 anomaly which is a small plateau in conductance around $(0.7-0.5)G_0$.[1] The behavior of this plateau as a function of temperature, magnetic field, and bias voltage has been intensively studied.[1–4]

There are several explanations for the 0.7 anomaly. In the Kondo model an unpaired electron is localized at the QPC.[5,6] The spin coupling to the electrons in the leads results in a high density of states, a Kondo resonance, at the Fermi level. This enhances conductance around the zero bias voltage. The Kondo model seemingly explains the conductance plateaus and their behavior as a function of temperature and external magnetic field.[5,6] Another explanation is provided by the semiempirical model by Reilly *et al.*[7] As the electron density at the QPC increases controlled by a gate voltage a spin gap opens and the electron gas polarizes. As a result a plateau around $(0.7-0.5)G_0$ is seen in the conductance.[7] The spin-polarization model has also been adopted by Berggren and Yakimenko[8] and Starikov *et al.*[9] They used density-functional theory (DFT) to calculate the electron density and the conductance as a function of the gate voltage for a realistic QPC model. In addition to the ground-state solution Starikov *et al.* found at certain gate voltages also metastable states which they used to interpret the temperature dependence of the 0.7 anomaly. Moreover, Meir *et al.*[6] and Hirose *et al.*[5] reported DFT calculations devoted to modeling the QPC resonance states needed in the Kondo model. Despite the common feature of the spontaneous spin polarization, the results of these DFT models vary remarkably. In this context, it is interesting to note that also recent measurements utilizing the resonant interaction between two QW's show evidence of localized moment formation in a 2D constriction.[10]

In this work we use DFT to investigate the spontaneous spin polarization and its consequences for the conduction in QW's. In contrast to the model Hamiltonian studies we can take the actual geometry and the effects of the gate potential directly into account. The use of the Green's function technique allows us to study real open systems with infinite electrodes even in the nonequilibrium case under a finite bias voltage. However, we keep the model geometry simple in order to obtain physically transparent results and we study to what extent the mean-field DFT model can describe the experimental findings. The previous papers have typically concentrated on one QPC or QW structure whereas we study systematically the influence of the QW geometry, the temperature, and the bias voltage.

Below we use in the equations effective atomic units which are derived by setting $e=\hbar=m_e=m^*=\epsilon=1$. m^* and ϵ are the relative effective electron mass and the relative dielectric constant, respectively. For GaAs $m^*=0.067$ and $\epsilon=12.7$ and the effective atomic units of length and energy are $a_0^*=10.0307$ nm and $Ha^*=11.3079$ meV, respectively. We use these relations to convert the model parameters and results to values comparable with real systems.

Our quasi-2D model for a QW is shown in Fig. 1. The calculation area Ω consists of the QW and parts of the elec-

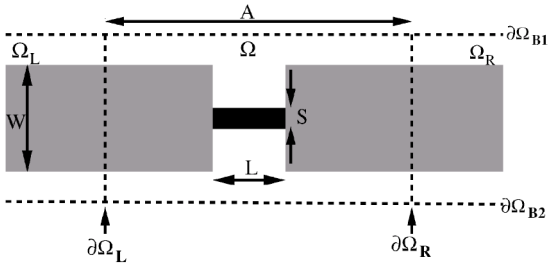

FIG. 1. 2D quantum wire between two electrodes. The gray areas denote the rigid positive background charge of the electrodes. The electrodes continue to infinity outside the calculation region. The uniform background charge density is varied in the black wire region in order to model the effects of the gate voltage.

trodes. The semi-infinite electrodes include the positive background charge with the constant density of $0.2(a_0^*)^{-2} \approx 2\times 10^{11} e/\mathrm{cm}^2$, which is a typical experimental value for the 2D electron gas at the interface, and the neutralizing 2D electron gas with the density $\rho(\mathbf{r})$. The electron density deep in the electrodes in the regions $\Omega_{L/R}$ is assumed to coincide with that in an infinite uniform wire. The QW between the electrodes is also modeled using a rigid uniform positive background charge (the black region in Fig. 1). We vary this positive charge density in order to mimic the effects of a gate voltage, i.e., we define the gate voltage as the Coulomb potential due to this charge at the midpoint of the QW. At both sides of the electrodes and the wire we include enough empty vacuum, and the electron density is required to vanish at the boundaries $\partial\Omega_{B1/B2}$.

We employ the DFT within the local density approximation[11] (LDA) for the electron exchange and correlation and calculate the electron density using Green's functions as

$$\rho(\mathbf{r}) = \frac{-1}{2\pi}\int_{-\infty}^{\infty} \mathrm{Im}[G^<(\mathbf{r},\mathbf{r};\omega)]d\omega. \tag{1}$$

Above, $G^<(\mathbf{r},\mathbf{r};\omega)$ is the so-called lesser Green's function and the integration is over all energy values. $G^<(\mathbf{r},\mathbf{r};\omega)$ has to be solved self-consistently with respect to the electron density and the effective potential and using open boundary conditions at $\partial\Omega_{L/R}$ (see, e.g., Ref. 12). The effective potential consists of the usual Coulomb potentials due to the positive and negative charge densities and the exchange-correlation potential within the LDA. It may also include a ramp potential which takes into account a possible bias voltage between the electrodes. The scheme is computationally much more demanding than solving for the wave functions of a finite system. However, it has the important advantages that finite-size effects are vanishingly small due to the open boundary conditions and that the effects of a finite bias are calculated self-consistently in nonequilibrium.

For a finite bias the electric current is calculated as

$$I = \frac{1}{\pi}\int_{-\infty}^{\infty} T(\omega)[f_L(\omega) - f_R(\omega)]d\omega, \tag{2}$$

where the Fermi functions f_L and f_R are shifted with respect to each other by the bias voltage V_{sd}. $T(\omega)$ is the tunneling probability and it is calculated using the Green's functions. In the zero-bias limit $f_L(\omega)=f_R(\omega)=f(\omega)$ and one obtains the linear-response conductance as

$$G = \frac{1}{\pi}\int_{-\infty}^{\infty} T(\omega)\frac{df(\omega)}{d\omega}d\omega. \tag{3}$$

At zero temperature the conductance is simply $T(\omega_f)$, where ω_f is the Fermi energy. At a finite temperature also electron states with energies near the Fermi level contribute to the conductance, as the derivative of the Fermi function $f(\omega)$ differs from the δ function. A finite temperature influences the solution also through the electron density. Below we show also differential conductances corresponding to given bias voltages at zero temperature. We determine them by increasing the bias voltage slightly and calculating the derivative dI/dV_{sd} numerically.

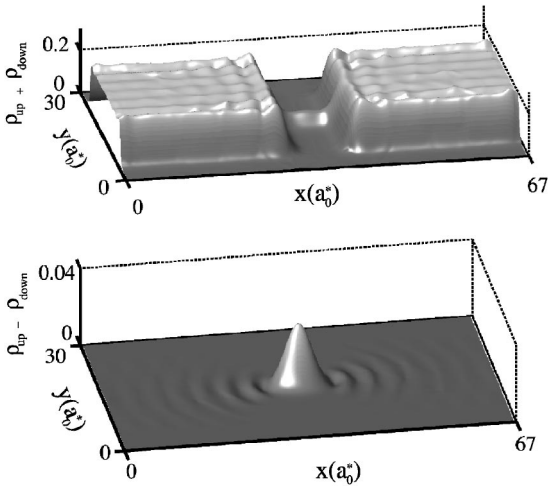

FIG. 2. (a) Total electron density and (b) difference between the spin-up and spin-down electron densities at zero temperature for a system with dimensions $S=5a_0^*$, $L=7a_0^*$, $W=20a_0^*$, $A=47a_0^*$ (see Fig. 1) and for the gate voltage of 12.4 mV.

We have implemented the nonequilibrium DFT scheme using the finite-element method as explained in our paper.[13] We use 2D high-order polynomial bases[14] up to the fourth order in order to reduce the basis size. In a typical calculation the number of basis functions needed to reach sufficient accuracy is ~2800 for high-order polynomials compared to ~5500 for low-order polynomials.

We have studied the electron structures of several QW's of different lengths $[L=(5-10)a_0^*]$ and widths $[S=(5-10)a_0^*]$ and determined their conductance as a function of the gate voltage. The width of the electrodes $W=20a_0^*$ used is clearly larger than those of the QW's. The widest QW's show the typical conductance staircase as a function of the gate voltage. For the narrowest QW's our model predicts prominent electron resonance states. They are evident as peaks in the local density of states (LDOS) (see Fig. 5 below). They can be thought to result as interference of the waves transmitted and reflected at the ends of the QW but, on the other hand, the resonances contain also characteristics of the DOS in quasi-one-dimensional wires. The resonance peaks are broader in short and wide QW's than in long and thin QW's, because short QW's are more strongly connected to the electrodes. If the resonance peaks are narrow enough, a spontaneous spin polarization occurs in a limited range of gate voltages. One solution with spin polarization in the QW is shown in Fig. 2 which gives the total electron density and the difference between the spin-up and spin-down densities. Meir *et al.*,[6] Berggren and Yakimenko,[8] and Starikov *et al.* have also found spin-polarized solutions in their DFT calculations for QPC's. They used models which correspond most closely to the shortest QW's of our calculations. The broad resonances found by Meir *et al.* and the nonappearance of the resonances in the calculation by Starikov *et al.* are therefore in agreement with the trend of our results.

Below we are concerned mainly with the conductance plateaus below $1G_0$ and therefore we discuss only narrow

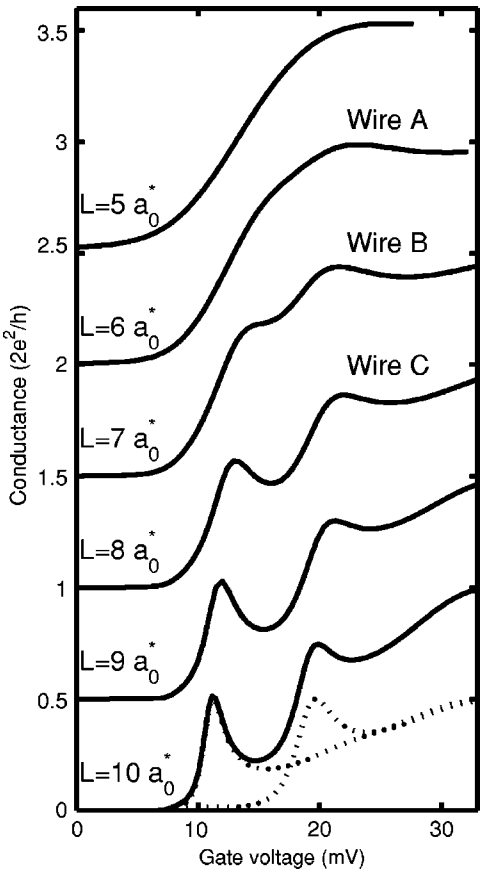

FIG. 3. Conductance as a function of the gate voltage for QW's with width $S=5a_0$ and with different lengths L. The width of the electrodes is $W=20a_0^*$, and the length of the computational area is $A=47a_0^*$ (see also Fig. 1). The successive curves have been shifted by $0.5G_0$. The conductance of the wire with $L=10a_0$ is decomposed into spin-up and spin-down contributions (dotted lines).

wires with width $S=5a_0^*$, where spontaneous spin polarization happens. The conductances of wires of different lengths L are shown in Fig. 3 as a function of the gate voltage and at zero temperature. The figure shows clearly the effect of the electrode-wire connection. The long wires have clear peaks due to resonances. The heights of the peaks are $0.5G_0$, meaning that only a single electron polarized mode contributes to them. The wires with lengths $L=(6-8)a_0^*$ exhibit resonances which are just narrow enough for the spin polarization to appear. The length dependence of the conductance among these three wires is in qualitative agreement with the recent measurements for QW's by Reilly *et al.*[3] That is, although the wires in the experiments are clearly longer than in our calculations, the structure around $(0.5-0.7)G_0$ becomes lower and forms a clear peak below $0.5G_0$ when the length of the wire increases. The differences between the experiment and theory may be due to the fact that in experiments side gates are used.[2] They control not only the potential level in the QW, but also the width of the QW.

The effect of the temperature on the conductance behavior of three QPC-like wires is shown in Fig 4. At zero temperature, wire A ($L=6a_0^*$) shows no plateau, whereas wire B ($L=7a_0^*$) has a plateau at $\sim 0.7G_0^*$ and wire C ($L=8a_0^*$) at

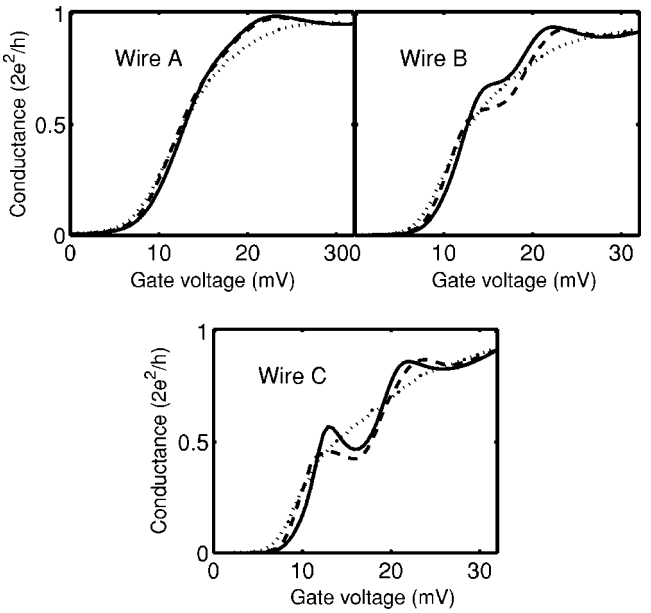

FIG. 4. Conductance as a function of the gate voltage for QW's with the width $S=5a_0^*$ and lengths $L=6a_0^*$ (wire A), $7a_0^*$ (wire B) and $8a_0^*$ (wire C) at the temperatures of 0 K (solid curve), 2 K (dashed curve), and 4 K (dotted curve).

$\sim 0.5G_0$. When the temperature increases the plateaus below $1G_0$ in wires B and C shift downward and become smoother. Wire A shows a weak temperature dependence so that the slope at $\sim 0.7G_0$ decreases. These findings are reminiscent of the experimental temperature dependences.[1,5]

The reason for the different temperature behaviors of the QW's in our model can be seen in Fig. 5 which shows the decomposition of the conductance of wire B into the spin-up and spin-down electron contributions at two different temperatures. As the temperature increases from 0 to 2 K spin polarization increases at the gate voltages around the middle of the plateau below $1G_0$. At the same time, the (resonance) peaks become also wider because more states contribute to the conductance [see Eq. (3)]. The same behavior is seen also for wires A and C. The reason for the increase in the polarization is seen in the LDOS for wire B in the lowest part of Fig. 5. When the temperature rises the electron density increases in the QW due to the resonances near the Fermi level. Then the decrease in the exchange-correlation energy opens the spin gap, as can be seen in Fig. 5, and the polarization increases. The effect is clearer for wire B than for wires A and C. In wire A the electron density does not increase as fast as in wire B because the resonance peaks are wider. Wire C has a strong polarization already at zero temperature and therefore it cannot show an increase as large as wire B.

Our analysis of the temperature behavior is to a certain extent parallel to the phenomenological model of Reilly *et al.*[7] In their model the relevant parameter is the ratio between the width of the spin gap and the thermal energy k_BT determining the occupancy of the discrete spin-up and spin-down energy levels. According to our calculations the temperature broadening in the Fermi functions is small when compared to the widths of the resonance peaks. Therefore k_BT has to be

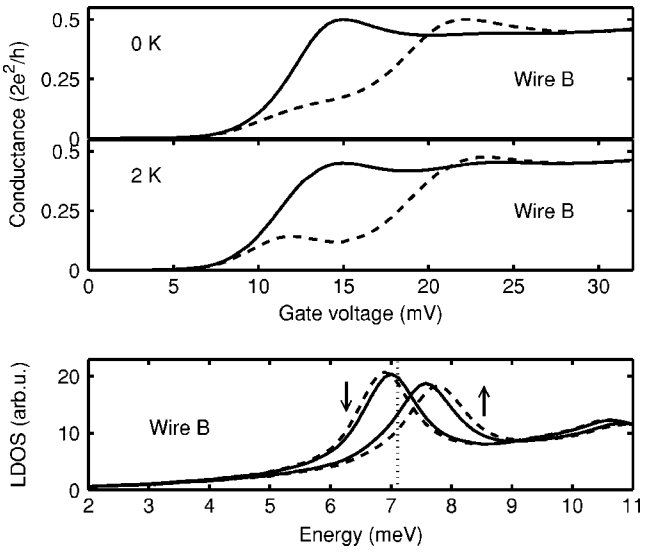

FIG. 5. Uppermost and middle panels: Conductances due to spin-up (dashed curves) and spin-down (solid curves) electrons as a function of the gate voltage and at temperatures of 0 and 2 K. Lowest panel: LDOS corresponding to the QW region for the spin-up and spin-down states at the gate voltage of 14 mV and at the temperatures of 0 K (solid curve) and 2 K (dashed curve). The dotted line denotes the Fermi level. The results are for wire B with the length $L=7a_0^*$.

replaced by the resonance peak width as the relevant parameter. Then the model can be used to explain the conductance–gate-voltage curves also at zero temperature.

The differential conductance of wire B at different bias voltages is shown in Fig. 6 as a function of the gate voltage. The increase in the applied bias voltage mainly increases the conductance but at the same time it also curtails the conductance plateaus. This is not exactly in agreement with the measurements, which show that the conductance plateau below $1G_0$ rises with increasing bias voltage.[4,5] According to

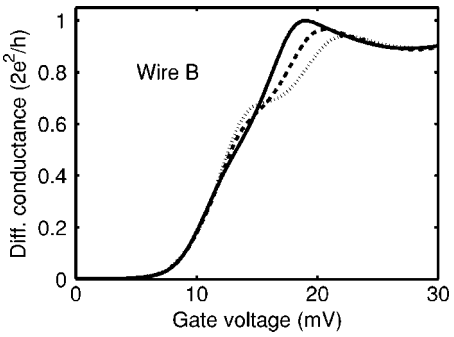

FIG. 6. Differential conductance of wire B with the width $S=5a_0^*$ and length $L=7a_0^*$ as a function of the gate voltage and at zero temperature. Results for bias voltages of 0 mV (dotted curve), 0.23 mV (dashed curve), and 0.46 mV (solid curve) are given.

our calculations the rise of V_{sd} diminishes also the spin polarization in the QW. Our model cannot give the zero-bias anomaly behavior seen in experiments and explained as a Kondo phenomenon.[5,6]

In conclusion, we have used density-functional theory and the Green's function method to model the electronic structures and conductances of quantum wires. The dependence of the conductance on the length of the wire as well as on the temperature and the bias voltage dependences are reminiscent of experimental findings. However, our mean-field approach cannot reproduce the zero-bias anomaly.

We acknowledge generous computer resources from the Center for Scientific Computing, Espoo, Finland. This research has been supported by the Academy of Finland through its Centers of Excellence Program (2000-2005). P.H. acknowledges financial support by the Vilho, Yrjö, and Kalle Väisälä Foundation. We have used the Harwell Subroutine Library in our calculations.

[1] K. J. Thomas *et al.*, Phys. Rev. Lett. **77**, 135 (1996); Phys. Rev. B **58**,4846 (1998).
[2] B. E. Kane *et al.*, Appl. Phys. Lett. **72**, 3506 (1998).
[3] D. J. Reilly *et al.*, Phys. Rev. B **63**, 121311 (2001).
[4] A. Kristensen *et al.*, Phys. Rev. B **62**, 10 950 (2000).
[5] S. M. Cronenwett *et al.*, Phys. Rev. Lett. **88**, 226805 (2002)
[6] Y. Meir *et al.*, Phys. Rev. Lett. **89**, 196802 (2002); K. Hirose *et al.*, *ibid.* **90**, 026804 (2003).
[7] D. J. Reilly *et al.*, Phys. Rev. Lett. **89**, 246801 (2002).
[8] K.-F. Berggren and I. I. Yakimenko, Phys. Rev. B **66**, 085323 (2002).
[9] A. A. Starikov *et al.*, Phys. Rev. B **67**, 235319 (2003).
[10] T. Morimoto *et al.*, Appl. Phys. Lett. **82**, 3952 (2003); V. I. Puller *et al.*, Phys. Rev. Lett. **92**, 096802 (2004); P. J. Bird and Y. Ochiai, Science **303**, 5664 (2004).
[11] C. Attaccalite *et al.*, Phys. Rev. Lett. **88**, 256601 (2002).
[12] Y. Xue *et al.*, Chem. Phys. **281**, 151 (2002).
[13] P. Havu *et al.*, Phys. Rev. B **69**, 115325 (2004).
[14] Ch. Schwab, *p- and hp-Finite Element Methods: Theory and Applications in Solid and Fluid Mechanics* (Oxford University Press, Oxford, 1998).